Int. J. Rock Mech. Min. Sci. & Geomech. Abstr. Vol. 13, pp. 149–154. Pergamon Press 1976. Printed in Great Britain

The Role of Asperity Indentation and Ploughing in Rock Friction—I.

Asperity Creep and Stick-Slip

C. H. SCHOLZ*
J. T. ENGELDER†

Two processes which produce the stick–slip instability in the frictional sliding of rock have been identified. These are: (1) fracture of asperities at the onset of sliding, and (2) creep at the sliding surface leading to a progressive increase in real area of contact with time. The second process produces an increase in friction with increased time of stationary contact or decreased sliding velocity, and results from stress corrosion cracking and/or hydrolytic weakening. The Bowden and Tabor *adhesion theory, when modified to include asperity creep, adequately predicts the frictional behavior of rock when brittle fracture of asperities is inhibited.*

INTRODUCTION

Over a broad range of pressure and temperature corresponding to the conditions of the upper part of the earth's lithosphere, rock exhibits an intermittent, jerky mode of frictional sliding known as stick–slip [1]. In nature, frictional sliding of faults also is thought to occur by stick–slip, resulting in earthquakes [2]. It is thus of some interest to understand the processes responsible for stick–slip friction of rock.

Stick–slip motion occurs as a result of an instability in which frictional resistance drops rapidly at the onset of sliding, or during sliding. If the drop in friction is more rapid than the unloading curve of the system loading the frictional element, stick–slip will occur.

Stick–slip friction in silicate rocks appears to be intimately connected with the indentation and ploughing of asperities. Rock typically slides stably at low normal stresses, and by stick–slip at high normal stresses [3]. Engelder [4] showed that quartzite and granite sliding surfaces always exhibit wear grooves resulting from asperity ploughing when sliding occurred by stick–slip, but do not have such grooves after stable sliding. The normal stress at the stable sliding to stick–slip transition thus appears to correspond to the normal stress that is sufficient to cause asperity indentation and ploughing. It seems logical, then, to look at ploughing phenomena as a source of the stick–slip instability.

Two mechanisms based on asperity behavior have been proposed to explain sliding of rock. The brittle fracture theory of stick–slip [3, 5] proposes that locked asperities fail by brittle fracture at the onset of sliding, thus resulting in a sudden drop in friction and consequent stick–slip. In support of this model, Byerlee [3] cited evidence for brittle fracture during sliding such as angular wear fragments and cracking in wear grooves. More direct evidence in favor of this model is that polished sliding surfaces that have undergone stick–slip typically show 'carrot' shaped wear grooves (Fig. 1). The sharp ends of these grooves point in the direction of motion of the surface in which the grooves lie, and the groove lengths are limited to the distance slipped during an individual stick–slip, rather than the total slip experienced [4, 6]. The formation of these grooves is thought to be due to ploughing, to an increasing degree, during stick–slip motion. The correlation of groove length and stick–slip displacement strongly suggests that groove producing asperities, which at the end of one stick–slip must lie at the blunt ends of the grooves, break off at the onset of the next stick–slip event.

A second mechanism that has recently been suggested as a mechanism of stick–slip friction in rock, is creep at the sliding surfaces which produces an increase in real area of contact, and hence static friction,

Fig. 1. Photomicrograph of typical 'carrot' shaped wear groove produced in stick–slip sliding of granite.

* Lamont-Doherty Geological Observatory of Columbia University, Palisades, NY 10964, U.S.A., also of the Department of Geological Sciences, Columbia University.
† Lamont-Doherty Geological Observatory of Columbia University, Palisades, NY 10964, U.S.A.

with time of stationary contact [7]. This mechanism was suggested by observations that the static coefficient of friction in rock increases with time of stationary contact [7–9]. Both the first and second mechanisms lead to a static coefficient of friction that is higher than the dynamic coefficient, and hence results in a stick–slip instability.

While we may regard the 'carrot' shaped grooves as incontrovertable evidence for brittle fracture at the onset of stick–slip in silicate rocks at room temperature, it is the purpose of this paper to demonstrate that the asperity creep mechanism also operates to produce stick–slip in rock and is responsible for the observed time dependence of rock friction. The influence of the relative hardness of asperity and substrate on ploughing and friction of rock is discussed in greater detail in the companion paper [pp. 155–163].

MICROINDENTATION EXPERIMENTS

Prior to discussing our friction results, we will first demonstrate that asperity creep does occur. We do this by considering the results of microindentation experiments in which a diamond indenter is viewed as a model of a hard asperity in stationary contact with a softer surface.

The experiments were done with a Leitz microindentation tester, equipped with a Vickers pyramidal diamond indenter. Two materials were tested, the rhomb $(10\bar{1}1)$ face of a natural quartz crystal from Herkimer Co., NY, and a crystal of olivine (of unknown orientation) in a polished section of Twin Sisters dunite. The experiments showed that for both materials the area of the indent increased with the duration of loading of the indenter. These results are shown in Fig. 2, where the area of indent is plotted as a function of loading duration. All experiments were done with a load of 25 g, and each data point is an average of about 25 individual measurements. The error bars indicate 98% confidence limits. These results show that the indent area increases approximately with log t. The coefficients obtained from the dashed line fits are given in the table.

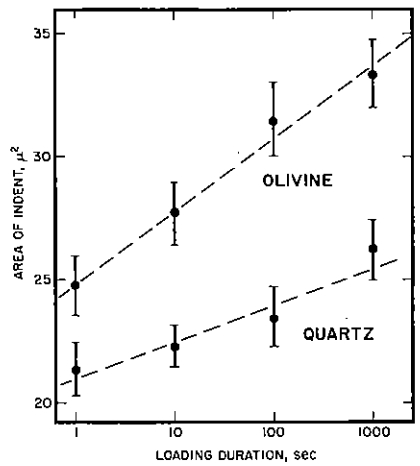

Fig. 2. Area of indent as a function of loading duration for quartz and olivine for Vickers microindentation experiments. Each data point is an average for about 25 individual measurements. The load was 25 g.

The above results, though the first to show that this phenomena occurs in silicates, are not particularly surprising, since Westbrook and Jorgensen [10] have shown that this behavior, termed indentation creep, is a property shared by a wide variety of nonmetallic materials. In MgO and LiF, it occurs by time dependent motion of dislocations [11], and Westbrook and Jorgensen [10, 12] have shown that it does not occur in a water-free environment. It thus appears to result from the hydrolytic reactions which produce stress–corrosion cracking in silicates and other nonmetals [13, 14] and in plastic deformation produces the phenomenon known as hydrolytic weakening [15]. Since indentation experiments are dominated more by plastic flow than by brittle fracture, the exact mechanism that results in indentation creep is probably hydrolytic weakening, though the two processes are analogous and may occur simultaneously.

The above results suggest that when two surfaces are placed in frictional contact under a normal force N, the asperities of the harder materials will gradually penetrate the softer surface through indentation creep. The real area of contact, A, will thus increase with time as, from Fig. 2

$$A = (1 + \alpha \log t)\frac{N}{P_1}, \tag{1}$$

where α is a constant, t is time in contact, and P_1 is the penetration hardness measured at unit time. Frictional sliding will then occur when

$$F = (1 + \alpha \log t)\frac{S}{P_1}N, \tag{2}$$

where S is the shear strength of the softer material, and F, the shear force. Therefore, the static coefficient of friction, μ_s will be time dependent, where

$$\mu_s = (1 + \alpha \log t)\bar{\mu}_s. \tag{3}$$

$\bar{\mu}_s$ is the friction coefficient at unit time of contact. Equation (3) satisfactorily agrees with the observed time dependence of friction of rock [7–9].

Although the semi-empirical model developed above applies to a situation in which hard asperities penetrate a softer substrate, the model is probably applicable to more general surfaces. In the case of a soft asperity contacting a harder surface, for example, the soft asperity is likely to flatten by creep, thus similarly increasing the contact area. For surfaces separated by wear particles, the contact area will increase by creep in the wear particles (or fault gouge) due to the same mechanism. In the next section we will explore how asperity indentation creep can lead to stick–slip in rock by describing some friction experiments designed to separate this process from the brittle fracture mechanism of stick–slip.

FRICTION EXPERIMENTS

Experimental procedures

In order to study the effects of asperity indentation creep on friction, it is necessary to devise a friction

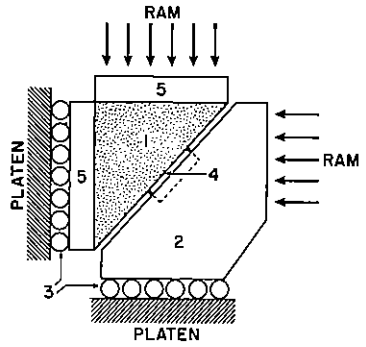

Fig. 3. Setup for friction experiments. (1) rock sample, (2) steel piece, (3) roller bearings, (4) sapphire disc and (5) steel endcap.

experiment which simulates as closely as possible the simple model of a hard asperity ploughing through a softer surface. The asperities must be sufficiently hard such that they do not break off at the onset of slip in order to allow that the indentation creep mechanism of stick–slip can be studied separately from the brittle fracture mechanism.

These conditions are achieved in an experiment in which rock is slid on a ground surface of synthetic sapphire. The sapphire, being much harder than any mineral in the rock, does not wear and therefore behaves in much the way the model is described. These experiments were performed in a biaxial loading frame (Fig. 3, also see Scholz *et al.*, [7] Fig. 1), in which the rock sample was a 30°–60°–90° triangular prism, 2.5 cm thick and 18 cm high. The opposing frictional surface was a 2.5 cm dia sapphire disc which was ground with a diamond wheel, and inset in a steel piece the same shape and size of the rock specimen. The vertical force is supplied by a hydraulic ram at 30° to the rock–sapphire interface and the horizontal force, by a ram at 60° to it.

Each experiment was conducted by pumping up both rams simultaneously until the normal stress across the frictional interface σ_n, was approx 50 bars. The horizontal ram was then sealed by means of a valve, and the vertical force increased with a constant volume-rate pump. As sliding commences, the horizontal ram compresses, leading to a continuous increase in σ_n. In these experiments, σ_n rose to about 500 bars after 1 mm of slip. The experiment was terminated at this point to avoid damage to the sapphire. The total slip that can be accommodated in the testing machine is 1 cm, which is here termed a 'run'. Approximately 10 experiments were conducted during each run. After each run the rock sample is reset to its original position, and another sequence of experiments started.

Observations

Each experiment was conducted at a constant sliding velocity, determined by the setting of the constant rate pump. In all cases, except for Solenhofen limestone, which will be discussed below, the rocks slid on the sapphire in a stable way, without stick–slip. Stick–slip only occurred if the experiment was interrupted and the rock allowed to rest in stationary contact with the sapphire. A single stick–slip then would initiate further sliding, after which stable sliding would resume.

This behavior is predicted from the model. Since the sapphire asperities do not break off, they plough at a depth which depends on the sliding velocity. Thus, the real area of contact for sliding at a velocity v is, by analogy with (3),

$$A = (1 - \beta \log v)\frac{N}{P_1}, \tag{4}$$

where β is a constant that depends on α and the asperity geometry. Therefore, the force required to cause sliding will be given by

$$F = (1 - \beta \log v)\frac{S}{P_1}N, \tag{5}$$

and the dynamic coefficient of friction defined as

$$\mu_d = (1 - \beta \log v)\bar{\mu}_d, \tag{6}$$

where $\bar{\mu}_d = S/P_1$. According to (5), friction will be constant at a constant sliding velocity and a stick–slip instability will not occur. If, however, sliding is halted and the surfaces held in contact for a time t' at a normal force N', an additional area of contact, A', will be produced by indentation creep, where

$$A' = (1 + \alpha \log t')\frac{N'}{P_1}. \tag{7}$$

If loading is resumed, ploughing must occur over the area $A + A'$, which will drop to A as sliding commences, resulting in a sudden reduction in friction which will cause stick–slip. The force necessary to initiate slip is therefore

$$F = \mu_d N + A'S, \tag{8}$$

where $\mu_d = (1 - \beta \log \bar{v})\bar{\mu}_d$ where $\bar{v}$ is the average sliding velocity during stick–slip.

Notice that dynamic friction (equation 5) obeys Amonton's law, whereas static friction obeys a Navier–Coulomb type law (equation 8) where $A'S$ is the 'cohesion' term. This is exactly the behavior exhibited by the rock–sapphire experiments. In Fig. 4 this is illustrated for Westerly granite on sapphire. In this experiment, as the vertical ram was advanced at a constant

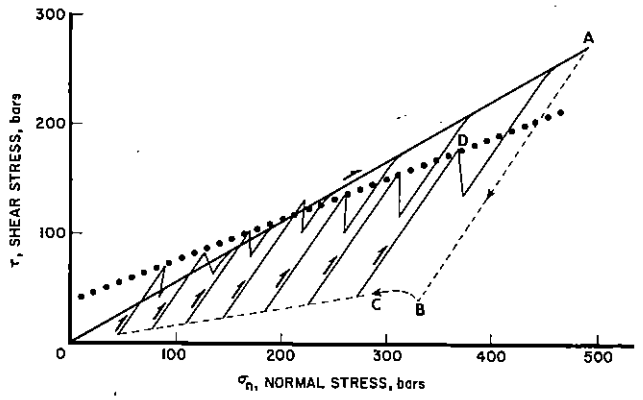

Fig. 4. Frictional behavior of Westerly granite sliding of sapphire. *OA* is the friction law for stable sliding at a velocity of 0.03 mm/sec. The dotted line is the friction law for the onset of stick–slips after the surfaces were held in stationary contact at point B for 300 sec.

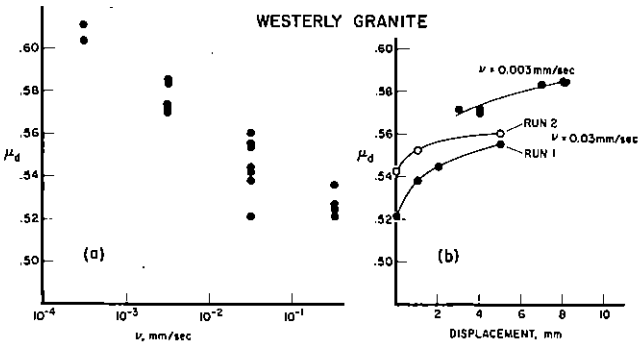

Fig. 5. Stable sliding behavior of Westerly granite on sapphite. (a) friction as a function of sliding velocity, (b) the same data, at two velocities, replotted as a function of cumulative sliding displacement.

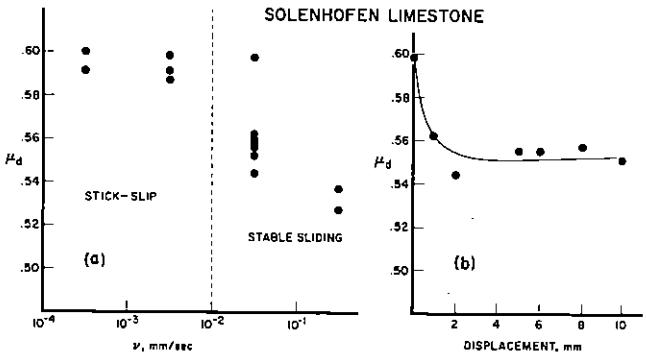

Fig. 7. Same as Fig. 5 for Solenhofen limestone. See text for explanation of stick–slip field.

velocity, stable sliding occurred at a constant velocity of 0.03 mm/sec, and the stresses followed the path OA, obeying Amonton's law. At A, sliding was stopped and the sample unloaded along AB to B, where the sample was held in stationary contact for 300 sec. The sample was then rapidly unloaded to C then loaded to D, at which point stick–slip occurred. Continued loading after stick–slip brought the stresses back to line OA, at which point stable sliding commenced. This procedure was repeated to produce stick–slip at a number of different values of σ_n. The dotted line is the locus of stresses at the onset of stick–slip, and is of the form predicted by equation (8). Also notice that the slope $(d\tau)/(d\sigma_n)$, for the dotted line is less than the slope OA for stable sliding. This is also predicted from equations (5) and (8), since the average velocity during stick–slip, $\bar{v}$, is much greater than v. Using a value of 0.07 for β and 0.51 for μ_d (determined below), we calculate $\bar{v}$ as 1–10 cm/sec in these experiments. This value is in accord with particle velocities measured directly during stick–slip of rock under similar conditions in this testing apparatus [16].

It is worth noting that Engelder [17] observed these same relationships between the friction laws for stable sliding and stick–slip of sandstone on quartz gouge. His observations were based on triaxial experiments at normal stresses up to 3.5 kbar.

Velocity dependence

The effect of sliding velocity on the dynamic coefficient of friction is shown for three rock types in Figs. 5–7. Each data point represents μ_d measured during an experiment in which approximately 1 mm of stable slip occurred as σ_n increased from 50 to 500 bars. Since Amonton's law was obeyed in these experiments, μ_d was a constant over this range of normal stress.

The velocity effect is clearly shown in Figs. 5a and 6a, for Westerly granite and Twin Sisters dunite, respectively. The observed constants are given in Table 1. The scatter in the data largely results from the effect of sliding displacement on friction. At the beginning of the first experimental run, the rock samples were ground with an 80 grit wheel. As sliding occurs, the resulting surface damage leads to a steady increase in μ_d. As a result, successive experiments at the same velocity show higher values of friction. In order to avoid biasing the data with this effect, the velocities of successive experiments were selected in a quasi-random way.

In Fig. 5b, the data at two velocities from Fig. 5a are replotted as a function of the cumulative displacement at the beginning of each experiment. The monotonic increase of μ_d with displacement appears to largely explain the scatter in Fig. 5a. Note that after 10 experiments, the rock was reset to its original position (without regrinding) and run 2 begun. At $v = 0.03$ mm/sec, the initial μ_d was slightly lower than its final value in run 1, but quickly rose to a high value as sliding proceeded.

The effect of displacement on friction for the dunite was so strong that the data in Fig. 6 has been separated into the two successive runs. The velocity dependence of μ_d, as predicted by equation (6) is clearly shown by this rock as well. In contrast, the frictional behavior of Solenhofen limestone differed markedly in several

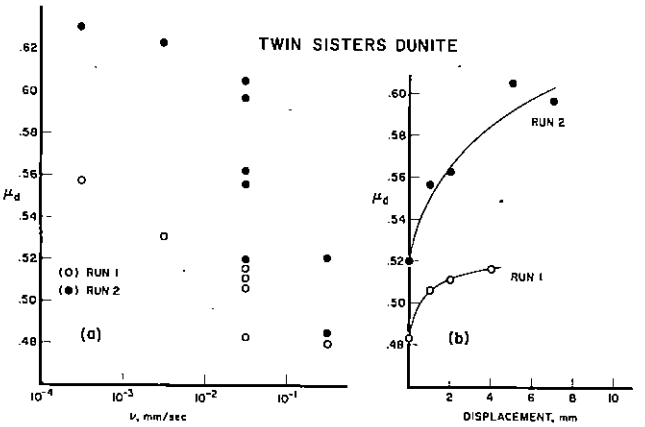

Fig. 6. Same as Fig. 5 for Twin Sisters dunite on sapphire.

TABLE 1. EXPERIMENTALLY DETERMINED PARAMETERS

Type of experiment	P_1 kg/mm^2	$\bar{\mu}_d$	α	β
Microindentation:				
quartz	1170 ± 45		0.08 ± 0.03	
olivine	1010 ± 40		0.13 ± 0.02	
Dynamic friction				
Westerly granite		0.51 ± 0.01		0.07 ± 0.01
Twin Sisters dunite (run 1)		0.48 ± 0.02		0.07 ± 0.02
Stick–slip stress drop				
Barre granite			0.10 ± 0.02	

respects from that of the dunite and granite (Fig. 7). Firstly, stable sliding occurred only for velocities greater than 10^{-2} mm/sec and it was also only in this range of velocity that the friction was velocity dependent. At slower velocities, sliding was by stick–slip, and friction was independent of velocity. Secondly, μ_d was observed to decrease with displacement, in contrast to the behavior of the silicate rocks. These differences would appear to be explained by the far greater softness of the limestone, which allows much deeper penetration of the sapphire asperities than in the dunite and granite. If we assume that the asperities are nearly fully penetrating, then the development of wear particles during sliding will tend to reduce penetration and hence friction will decrease with displacement, as observed. Also, if asperities are fully penetrated, the real area of contact will be large and penetration creep will be inhibited, and further, any motion will tend to reduce that penetration, resulting in a stick–slip instability. The behavior of Solenhofen limestone at velocities below 10^{-2} mm/sec thus can be explained by nearly total asperity penetration.

This line of reasoning would lead us to suggest that at much higher normal stresses (or slower velocities) the dunite and granite will also be expected to undergo a similar transition to stick–slip as full asperity penetration is approached.

One further comment should be made regarding these results. Equation (6) is simply a modification of the adhesion theory of friction [18] to account for asperity indentation creep. It follows from (6) that μ_d at a given velocity is simply proportional to S/P_1. Since both S and P_1 are strength properties of the same (softer) material, it is likely that they will vary together with diverse materials, hence μ_d should not be expected to vary with different materials. This accounts for the very similar values of μ_d obtained for the three rock types discussed above.

Stick–slip

If we rewrite equation (8) in terms of stresses, we have

$$\tau_1 = \mu_d \sigma_n + \frac{A'}{A_t} S, \tag{9}$$

where τ_1 is the shear stress at the onset of stick–slip, σ_n the normal stress, and A_t is the total area of the surface.

If we neglect elastic radiation [7], the stress-drop during stick–slip, $\Delta\tau = 2(\tau_1 - \tau_f)$, where $\tau_f = \mu_d \tau_n$. If we do an experiment then, as is shown in Fig. 4, in which the sample is held in stationary contact for a time t', at a stress σ_n, the stress drop of the ensuing stick–slip will be given using (7) and (9), by

$$\Delta\tau = 2\frac{A'}{A_t} S = 2(1 + \alpha \log t')\frac{S}{P_1}\sigma_n'. \tag{10}$$

A series of experiments in which Westerly granite was held in stationary contact with sapphire at different values of t' and σ_n' and subsequently stick–slipped, are shown in Fig. 8. These results substantially agree with

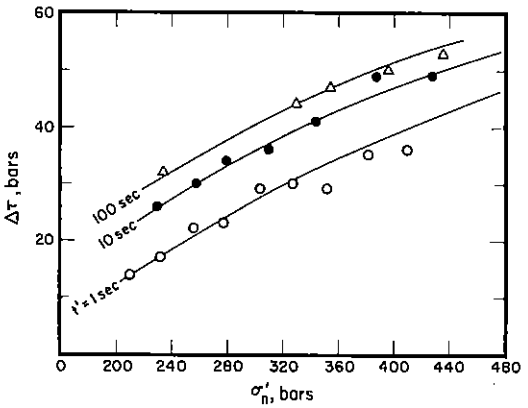

Fig. 8. The stress drop for stick–slips which followed stationary contact for the t' at normal stress σ_n' for Westerly granite on sapphire.

equation 10. The slight divergence from (10) shown in Fig. 8 can be explained if the elastic radiation efficiency increases slightly with stress drop, which will decrease $\Delta\tau$ from the value given by the RHS of (10) [7].

In Fig. 9, we show data taken over a broader range of t', at $\sigma_n' = 200$ bars, for Barre granite on sapphire. Here the stress-drops are normalized to the value for $t' = 3$ sec for each run, to reduce scatter due to displacement effects. These results verify the expected logarithmic dependence at $\Delta\tau$ on t', and agree quantitatively with the quartz indentation creep results shown in Fig. 2. The constant α for indentation creep of quartz is 0.08 ± 0.03 and for Barre granite friction, from Fig. 9 and equation 10, $\alpha = 0.10 \pm 0.02$. These are listed, together with the other experimentally determined parameters, in Table 1.

CONCLUSIONS

In this paper, we have studied the role of asperity indentation creep in the friction of rock by conducting experiments designed to isolate this phenomena from other processes, namely brittle fracture of asperities, which may otherwise complicate the frictional behavior.

As a result we have found that this mechanism is responsible for the various time and velocity dependent

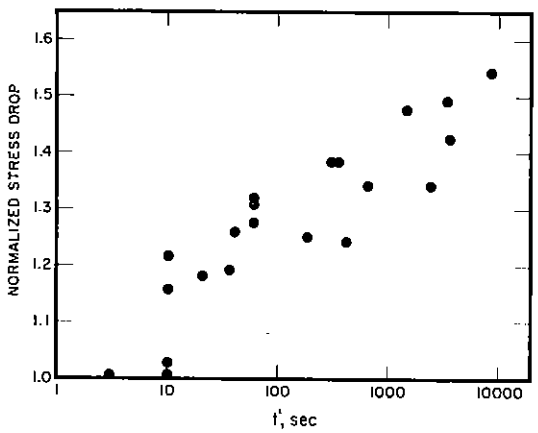

Fig. 9. Stress drops for stick–slips which followed stationary contact for time t' at $\sigma_n' = 200$ bars for Barre granite on sapphire. These stress drops are normalized to the stress drop at $t' = 3$ sec for each of several runs.

properties of rock friction. We have further shown that a simple model, based on Bowden and Tabor's [18] adhesion theory, modified to take indentation creep into account, adequately predicts the observed frictional behavior. We have seen, however, that this model breaks down when the materials in contact have an extreme hardness contrast, as with limestone sliding on sapphire. This has led us to make a more detailed study of the important effect of hardness contrast on the mode of frictional sliding. This work is the subject of the companion paper.

Asperity indentation creep and its attendant frictional effects leads to a physical understanding of the difference between static and dynamic friction in rock. It is shown to be an important mechanism for stick–slip sliding.

Acknowledgements—This work was supported by NSF grants GA36357 and GA43295. We thank Professor G. Kehl for allowing us the use of the microindentation tester, and L. Sykes, P. Richards and R. Anderson for critically reviewing the text. Lamont-Doherty Geological Observatory Contribution No. 2336.

Received 5 *November* 1975.

REFERENCES

1. Byerlee J. D. & Brace W. F. Stick–slip, stable sliding and earthquakes. *J. Geophys. Res.* **93,** 6031 (1968).
2. Brace W. F. & Byerlee J. D. Stick–slip as a mechanism of earthquakes. *Science* **153,** 990 (1966).
3. Byerlee J. D. Theory of friction based on brittle fracture. *J. appl. Phys.* **38,** 2928 (1967).
4. Engelder J. T. Effect on scratch hardness on frictional wear and stick–slip on Westerly granite and Cheshire quartizite. In *The Physics and Chemistry of Rocks and Minerals.* Proc. NATO Study Conference on petrophysics, Newcastle (1974). To be published.
5. Byerlee J. D. The mechanism of stick–slip. *Tectonophysics* **9,** 475 (1970).
6. Engelder J. T. Microscopic wear grooves on slickensides: indicators of paleoseismicity. *J. Geophys. Res.* **79,** 4387 (1974).
7. Scholz C. H., Molnar P. & Johnson T. Detailed studies of frictional sliding of granite and implications for the earthquake mechanism. *J. Geophys. Res.* **77,** 6392 (1972).
8. Dieterich J. H. Time-dependent friction in rocks. *J. Geophys. Res.* **20,** 3690 (1972).
9. Stetsky R. M., Brace W. F., Riley D. K. & Robin P. F. Friction in faulted rock at high temperature and pressure. *Tectonophysics* **23,** 117 (1974).
10. Westbrook J. H. & Jorgensen P. J. Indentation creep of solids. *Trans. Met. Soc. AIME* **233,** 425
11. Walker W. W. & Demer L. J. Effect of loading duration on indentation hardness. *Trans. Met. Soc. AIME* **230,** 613 (1964).
12. Westbrook J. H. & Jorgensen P. J. Effects of water desorption on indentation microhardness anisotrophy in minerals. *Am. Mineral.* **53,** 1899 (1968).
13. Scholz C. H. Static fatigue of quartz. *J. Geophys. Res.* **77,** 2104 (1972).
14. Martin R. J. Time dependent crack growth in quartz and its application to the creep of rocks. *J. Geophys. Res.* **77,** 1406 (1972).
15. Griggs D. T. & Blacic J. D. Quartz: anomalous weakening of synthetic crystals. *Science* **147,** 292 (1965).
16. Johnson T. & Scholz C. H. The dynamic properties of stick–slip friction of rocks. *J. Geophys. Res.* **81,** 881 (1976).
17. Engelder J. T. Coefficients of friction for sandstone sliding on quartz gouge. *Advances in Rock Mech., Proc. Third Cong. Int. Soc. Rock Mech. Denver,* part A, 499 (1974).
18. Bowden F. P. & Tabor D. *The Friction and Lubrication of Solids.* pp. 79–82. Clarenden Press, Oxford (1950).